ISSN 0023-1584, Kinetics and Catalysis, 2020, Vol. 61, No. 6, pp. 894–902. © Pleiades Publishing, Ltd., 2020.
Russian Text © The Author(s), 2020, published in Kinetika i Kataliz, 2020, Vol. 61, No. 6, pp. 864–872.

# Effect of Promoter M (M = Au, Ag, Cu, Ce, Fe, Ni, Co, Zn) on the Activity of Pd–M/$Al_2O_3$ Catalysts of Ethanol Conversion into α-Alcohols

**S. A. Nikolaev[a, *], M. V. Tsodikov[b], A. V. Chistyakov[b], P. A. Chistyakova[b], D. I. Ezzhelenko[a], and I. N. Krotova[a]**

[a] *Faculty of Chemistry, Moscow State University, Moscow, 119991 Russia*

[b] *Topchiev Institute of Petrochemical Synthesis, Russian Academy of Sciences, Moscow, 119991 Russia*

**e-mail: serge2000@rambler.ru*

Received February 17, 2020; revised April 23, 2020; accepted May 4, 2020

**Abstract**—Pd/$Al_2O_3$ and Pd–M/$Al_2O_3$ catalysts (M = Au, Ag, Cu, Ce, Fe, Ni, Co, Zn) were obtained by ion exchange and impregnation. Pd/$Al_2O_3$ had high initial activity in the conversion of ethanol into α-alcohols, but lost 90% of its activity after 10 h of operation because of deactivation caused by the chemisorption of the by-product (CO) on Pd atoms. Modification of Pd with gold or silver led to an increase in the rate of Pd deactivation. As a result, the Pd–Au and Pd–Ag systems were less active and stable. In contrast, the Pd–Fe, Pd–Co, Pd–Ni, Pd–Cu, Pd–Zn, and Pd–Ce systems exhibited higher resistance to CO poisoning than Pd and demonstrated high activity and stability. The observed tendencies in the catalytic action of the mono- and bimetallic systems were explained within the framework of the *d* band model proposed by Hammer and Norskov. Pd–Cu/$Al_2O_3$ was most effective in the target process; it is not poisoned by CO and allows ethanol conversion into α-alcohols at 95% selectivity, while the time of its stable operation is at least 100 h. The structure of the Pd–Cu catalytic system was studied by TEM, EDA, XPS, TPR-$H_2$, and TPD-$NH_3$. A model of active catalyst sites was proposed.

*Keywords:* Pd–M, Pd–Cu, nanoparticles, catalysis, ethanol, α-alcohols

**DOI:** 10.1134/S0023158420060117

## INTRODUCTION

The development of technologies for conversion of biomass for the production of energy carriers and synthetic hydrocarbons has attracted the attention of scientists long ago [1, 2]. The production of ethanol (bioethanol) from biomass, used as an additive to motor fuel, is the best developed process in this direction [3]. According to the US Department of Energy, the global surplus in bioethanol production in 2016 was 10 million tons per year and continues to grow. Thus, bioethanol can be regarded as a promising raw material for the development of new technologies for the synthesis of valuable products on its basis.

One of the promising processes for conversion of ethanol into valuable products is a catalytic reaction leading to the formation of linear α-alcohols (butanol, hexanol, octanol) by condensation of the hydrocarbon skeleton of ethanol at 250–300°C [1, 2]. According to the data of [1–4], butanol forms via a chain of reactions: dehydrogenation of ethanol to ethanol, condensation of two ethanal molecules into 2-but-2-enal, and hydrogenation of 2-but-2-enal to butanal followed by hydrogenation of butanal to butanol (Scheme 1). Hexanol and octanol form by a similar mechanism. The by-products of ethanol conversion into α-alcohols are ethoxyethane, methane, and carbon monoxide (Scheme 1).

The highest activity in the catalytic conversion of ethanol into α-alcohols is shown by bifunctional systems $M^0/Al_2O_3$ (M = Pd, Pt, Ni, Cu, etc.), in which the metal is the catalyst of hydrogenation–dehydrogenation of reaction intermediates and the acid-base sites of alumina catalyze the condensation of ethanal into 2-but-2-enal. The efficiency of these systems was considered in reviews [2–5]. Some important data are shown below. Marcu et al. studied the activity of M/MgO–$Al_2O_3$ (M = Pd, Ag, Cu, Fe, and Sm) systems in ethanol conversion at 200°C [6]. The best process performance was achieved using the 5% Pd/MgO–$Al_2O_3$ catalyst (ethanol conversion 12%; selectivity for α-alcohols 72%). Riittonen et al. studied the activity of M/$Al_2O_3$ systems (M = Pd, Pt,

**Abbreviations and notation**: TEM, transmission electron microscopy; EDA, energy dispersive analysis; XPS, X-ray photoelectron spectroscopy; TPR-$H_2$, temperature-programmed reduction with hydrogen; TPD-$NH_3$, temperature-programmed desorption with ammonia; AAS, atomic absorption spectrometry.

Ru, Rh, and Ni) in ethanol conversion at 250°C [7]. The most effective catalyst was 20% $Ni/Al_2O_3$ (25% conversion, 80% selectivity). It was noted, however, that the $Ni/Al_2O_3$ systems showed low stability of operation during long-term experiments because of being deactivated during the reaction [7].

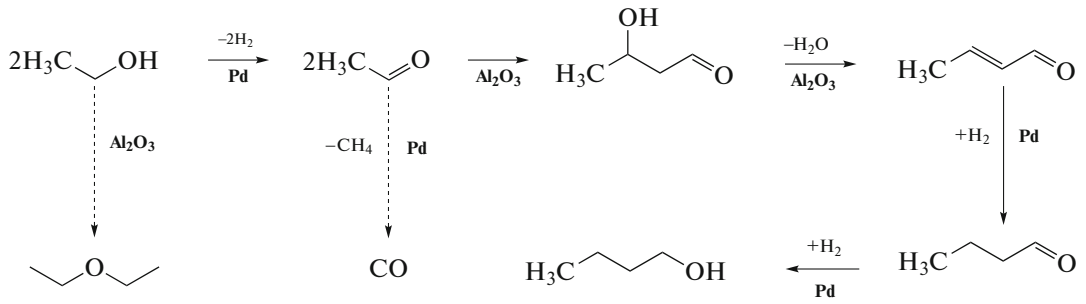


**Scheme 1.** Condensation of ethanol into butanol-1 on the $Pd/Al_2O_3$ bifunctional catalyst at 275°C (solid arrows). Side processes: decarbonylation on Pd sites and dehydration of ethanol on $Al_2O_3$ acid sites (dashed arrows). The data of [1–5, 8, 11].

Quick deactivation of monometallic catalysts for ethanol conversion into α-alcohols was also revealed in a kinetic study of the process on 0.1% $Pd/Al_2O_3$ [8]. The activity of the $Pd/Al_2O_3$ sample in the target process was high during the first 2 h of reaction, but drastically decreased in the next 3 h and became comparable to the activity of unmodified $Al_2O_3$. Consequently, the active Pd sites ceased to participate in catalysis with time. It was also found that in the presence of $Pd/Al_2O_3$, the target process was accompanied by decarbonylation (Scheme 1) with liberation of CO, whose chemisorption on Pd led to the formation of stable Pd–CO complexes [9, 10]. In this case, the fraction of active Pd sites available for ethanol sorption evidently decreased, resulting in a decrease in the process rate. It was assumed that the Pd component of the catalyst for ethanol conversion was deactivated because of CO chemisorption [8].

The goal of the present study was to develop new catalysts for the conversion of ethanol into α-alcohols steadily working in CO. For this purpose, we studied the effect of M promoters on the activity of Pd in 0.1% $Pd–M/Al_2O_3$ model catalysts (M = Au, Ag, Cu, Ce, Fe, Ni, Co, Zn).

The choice of promoters was dictated by two factors. First, $M/Al_2O_3$ catalysts are less active in the synthesis of α-alcohols compared with $Pd/Al_2O_3$ [11, 12], which makes it possible to correlate the activity of $Pd–M/Al_2O_3$ exactly with that of Pd atoms in bimetallic systems. Second, the metals (M) are modifiers of the electronic structure of Pd, which, according to [13–15], shift the center of the Pd *d* band relative to the Fermi level: Pd–Co (−3.2 eV) < Pd–Fe (−3.1 eV) < Pd–Ni (−2.8 eV) < Pd–Cu (−2.5 eV) < Pd–Zn (−2.45 eV) < Pd–Ce (−2.3 eV) < Pd (−1.8 eV) < Pd–Au (−1.6 eV) < Pd–Ag (−1.5 eV). As is known, the shift of the center of the Pd *d* band from the Fermi level leads to a decrease in the energy of binding of CO with Pd, and, vice versa, as a result of the shift of the center of the Pd *d* band to the Fermi level, this binding energy increases [13, 16]. Thus, the $Pd–Fe/Al_2O_3$, $Pd–Co/Al_2O_3$, $Pd–Ni/Al_2O_3$, $Pd–Cu/Al_2O_3$, $Pd–Zn/Al_2O$, and $Pd–Ce/Al_2O_3$ systems should have greater resistance to CO poisoning and demonstrate stable and high activity in the conversion of ethanol into α-alcohols, while $Pd–Au/Al_2O_3$ and $Pd–Ag/Al_2O_3$ should be less resistant to CO poisoning and exhibit lower activity compared with $Pd/Al_2O_3$.

## EXPERIMENTAL

The catalyst precursor $Pd/Al_2O_3^*$ (0.1 wt % Pd) was prepared by precipitation from a Pd nitrate solution [17]. For this, a $Pd(NO_3)_2 \cdot 2H_2O$ sample containing $4.7 \times 10^{-4}$ mol of Pd was dissolved in water (150 mL). The pH of solution was brought to 7.0 using 0.1 M NaOH, and the support (50 g, $\gamma$-$Al_2O_3$, $S_{sp}$ = 160 $m^2/g$, granule size 0.5 mm) calcinated at 350°C was added. The resulting suspension was stirred at 70°C for 1 h. The solution became discolored during the stirring, and the $Al_2O_3$ granules turned brown, indicating the deposition of Pd on the support surface. Then the granules were washed with water (5 L), dried, and calcinated at 350°C for 1 h.

The $Pd/Al_2O_3$ catalyst (0.1 wt % Pd) was obtained by calcinating $Pd/Al_2O_3^*$ at 350°C for 2 h with subsequent reduction with $H_2$ at 200°C for 2 h. The $Pd–M/Al_2O_3$ catalysts (M = Au, Ag, Cu, Ce , Fe, Ni, Co, Zn) were prepared by incipient wetness impregnation of $Pd/Al_2O_3^*$ [17, 18]. In a typical synthesis, an aqueous solution of metal nitrate (4.5 mL) containing an amount of metal equimolar to that of palladium was added to $Pd/Al_2O_3^*$ (5 g). After impregnation of $Pd–M/Al_2O_3$, it was dried and calcinated at 350°C for 2 h. Before testing, the $Pd–M/Al_2O_3$ catalysts were reduced with $H_2$ at 200°C for 2 h.

The metal content in the reduced samples was determined by atomic absorption spectrometry (AAS) on a Thermo iCE 3000 instrument (Thermo Fisher Scientific, United States). The relative error in measuring the metal content by this method did not exceed 1% [19, 20]. The actual Pd content in the catalysts was 0.1 wt %. The Pd : M molar ratio in the bimetallic catalysts was close to 1 : 1.

The micrographs of the reduced samples were obtained by transmission electron microscopy (TEM) on a JEM 2100F/UHR device (JEOL, Japan) with a resolution of 0.1 nm. The average particle size was determined by processing the data for 200–250 particles [21, 22]. The particle composition was identified by energy dispersive analysis (EDA) on a JED-2300 instrument (JEOL, Japan).

The X-ray photoelectron spectra of metals in the reduced samples were recorded on an Axis Ultra DLD spectrometer (Kratos Analytical, Great Britain; monochromatic Al$K_\alpha$ radiation, 1486.6 eV). The spectra were recorded using an electron gun to compensate for the static charge on the catalyst pellets. The spectra were recorded with an analyzer transmission energy of 40 eV at a step of 0.1 eV. To calibrate the energy scale, we used an external standard—gold foil with an electron binding energy of $E_{bnd}(\mathrm{Au}4f_{5/2}) = 83.96 \pm 0.03$ eV.

The unreduced catalysts were studied using temperature-programmed reduction with hydrogen (TPR-$H_2$) on a USGA-101 chemisorption analyzer (UNISIT, Russia). A 0.1 g sample was placed in a quartz reactor and calcinated in an argon flow (feed rate 20 mL/min) at 400°C for 1 h. The sample was cooled to 60°C, the argon flow was replaced by a mixture of 5% $H_2$ + 95% Ar (feed rate 30 mL/min), and the sample was heated at a rate of 10°C/min. Hydrogen absorption was recorded with a thermal conductivity detector.

The acidity of the reduced samples was measured using temperature-programmed desorption of $NH_3$ (TPD-$NH_3$) on a USGA-101 chemisorption analyzer [23]. For this, the sample (0.2 g) was placed in a quartz reactor and calcinated in a He flow (feed rate 20 mL/min) at 400°C for 1 h. The reactor was cooled to 25°C, and the sample was saturated with ammonia vapor for 30 min. The physically adsorbed forms of ammonia were removed by calcinating in a He flow at 100°C for 1 h. Then the sample was linearly heated at a rate of 8°C/min to 750°C in a helium flow (feed rate 30 mL/min). The released ammonia was recorded using a thermal conductivity detector.

The catalytic tests were performed on a Parr 5000 Series autoclave unit (Parr Instrument Company, United States) at a previously selected optimum temperature of 275°C [11, 24]. In the standard test cycle, ethanol (25 mL) and reduced catalyst (5 g) were placed in the reactor. The reactor was heated to 275°C, and the reaction medium was vigorously stirred for 5 h. Then the reactor was cooled to 25°C and opened, and qualitative and quantitative analysis of reaction products was performed.

The reaction products were analyzed by gas chromatography: gaseous $C_1$–$C_5$ hydrocarbons, on a Kristall-4000M chromatograph (Meta-Khrom, Russia, flame ionization detector, HP-PLOT column); CO, $CO_2$, and $H_2$, on a Kristall-4000 chromatograph (Meta-Khrom, Russia, thermal conductivity detector, SKT column). The qualitative composition of liquid organic products was determined by chromato-mass spectrometry on MSD 6973 (Agilent Technologies, United States, flame ionization detector, HP-5MS column) and Automass-150 (Delsi Nermag, France, flame ionization detector, CPSil-5 column) instruments with $E_I = 70$ eV. The contents of liquid organic substances were determined by gas-liquid chromatography on a Varian 3600 instrument (Varian, United States, Chromatek SE-30 column, 0.25 × 250 cm, $D$f = 0.3 mm, 50°C (5 min), 10 deg/min, 280°C, $t_{inj}$ = 250°C, split ratio 1/200, FID, *n*-octane as internal standard).

The ethanol conversion (α) was determined by the equation

$$a = (C_2H_5OH)_{fin} \times (C_2H_5OH)_{st}^{-1} \times 100\%,$$

where $(C_2H_5OH)_{fin}$ is the amount of ethanol in the reaction products, mol; and $(C_2H_5OH)_{st}$ is the amount of the starting ethanol, mol.

The amount of gaseous products ($n_i$, mol) was calculated by the equation

$$n_i = C_i V_g / 22.4,$$

where $C_i$ is the volume fraction of the *i*th component in the gas phase; $V_g$ is the volume of gases released during the reaction; and 22.4 is the molecular volume of the gas.

The amount of liquid products ($l_i$, mol) was calculated by the equation

$$l_i = C_i m_l M_i^{-1},$$

where $C_i$ is the mass fraction of the *i*th component in the liquid phase; $m_l$ is the total mass of liquid products, g; and $M_i$ is the molecular mass of the *i*th component.

The selectivity of formation of the *i*th component ($S_i$) was calculated by the equation

$$S_i = 0.5 \times I \times k_i \times [(C_2H_5OH)_{st} - (C_2H_5OH)_{fin})]^{-1},$$

where $I$ is the number of C atoms in the molecule of the *i*th component; $k_i$ is the number of moles of the *i*th component, mol; and $[(C_2H_5OH)_{st} - (C_2H_5OH)_{fin}]$ is the amount of alcohol involved in the reaction, mol.

The total yield of the products (ω, %) was calculated by the equation $\omega = a \times (S_1 + S_2 + S_2)$, where α is the conversion of ethanol, $S_1$ is the butanol selectivity, $S_2$ is the hexanol selectivity, and $S_3$ is the octanol selectivity.

**Table 1.** Catalytic characteristics of ethanol conversion into α-alcohols in the presence of the catalysts containing 0.1% Pd*

| Catalyst | Cycle | α, % | $S_1$, % | $S_2$, % | $S_3$, % | ω, % |
|---|---|---|---|---|---|---|
| $Pd/Al_2O_3$ | 1 | 24 | 65 | 3.6 | 0 | 16.5 |
| $Pd/Al_2O_3$ | 2 | 11.4 | 9.5 | 0.3 | 0 | 1.1 |
| $Pd/Al_2O_3$ + CO** | 1 | 12 | 8 | 0.5 | 0 | 1.0 |
| $Pd–Ag/Al_2O_3$ | 1 | 11.5 | 30 | 3 | 2 | 4.0 |
| $Pd–Ag/Al_2O_3$ + CO** | 1 | 7.4 | 2 | 0.1 | 0 | 0.2 |
| $Pd–Au/Al_2O_3$ | 1 | 16 | 50 | 2.5 | 0 | 8.4 |
| $Pd–Ce/Al_2O_3$ | 1 | 32 | 64 | 4 | 0 | 21.8 |
| $Pd–Zn/Al_2O_3$ | 1 | 59 | 53 | 10 | 1 | 37.8 |
| $Pd–Cu/Al_2O_3$ | 1 | 45.6 | 69.5 | 19 | 0 | 40.4 |
| $Pd–Cu/Al_2O_3$ + CO** | 1 | 41 | 73 | 19 | 2 | 38.5 |
| $Pd–Cu/Al_2O_3$ | 20 | 40.4 | 72 | 20 | 3 | 38.8 |
| $Pd–Ni/Al_2O_3$ | 1 | 29 | 73 | 10 | 2 | 24.7 |
| $Pd–Fe/Al_2O_3$ | 1 | 33 | 70 | 9.6 | 2 | 26.9 |
| $Pd–Co/Al_2O_3$ | 1 | 32 | 70 | 9 | 5 | 26.9 |
| $Pd–Co/Al_2O_3$ + CO** | 1 | 31.4 | 69.3 | 9 | 4 | 25.8 |

α is the ethanol conversion; $S_1$, $S_2$, and $S_3$ are the selectivities of formation of butanol, hexanol, and octanol, respectively; and ω is the total yield of products. Conditions of the standard test cycle: 275°C, 5 h, 5 g of catalyst, and 30 mL of ethanol.

* At 275°C the product yield in the presence of the 0.1%$M/Al_2O_3$ catalysts is less than 1% [11].

** The amount of CO added to the autoclave with the catalyst and ethanol was $1 \times 10^{-4}$ mol.

## RESULTS AND DISCUSSION

### *Activity of $Pd/Al_2O_3$*

Before describing the efficiency of bimetallic catalysts, it is necessary to briefly discuss the tendencies in ethanol conversion in the presence of the unmodified $Pd/Al_2O_3$ catalyst.

According to Table 1, the total selectivity for α-alcohols in the first cycle of testing of $Pd/Al_2O_3$ is 68.8 at 24% conversion of ethanol. Accordingly, the yield of α-alcohols on $Pd/Al_2O_3$ is 16.5%. However, already in the second cycle of testing, the product yield on $Pd/Al_2O_3$ decreased drastically to 1.1%. The yield decreased mainly because of the decrease in the selectivity of formation of α-alcohols. This result indicates that the rate of the target process is inhibited (Scheme 1).

According to [8], the catalytic poison for Pd-containing catalysts for ethanol conversion into linear α-alcohols is CO, which forms as a result of decarbonylation of ethanal (Scheme 1) and is tightly bonded to the active Pd sites. To test the applicability of the hypothesis about catalyst poisoning with CO under the given conditions, we analyzed the gas medium after the first cycle of testing of $Pd/Al_2O_3$. It turned out that CO was actually present in the products, and its amount formed in the first cycle was $5.2 \times 10^{-5}$ mol, which is comparable to the total amount of palladium in the $Pd/Al_2O_3$ sample. This result is consistent with the mechanism of catalyst poisoning as a result of CO chemisorption.

To directly test the effect of CO on the catalytic conversion of ethanol into α-alcohols, an experiment with a "poisoned catalyst" was performed. CO ($1 \times 10^{-4}$ mol) was added to an autoclave with the starting $Pd/Al_2O_3$ and ethanol. Then a standard test cycle was performed, and the composition of products was analyzed. According to Table 1, already in the first cycle, the yield of products on the Pd catalyst poisoned before the reaction was lower than during ethanol conversion in the presence of the initial Pd sample (Table 1, $Pd/Al_2O_3$ + CO, cycle 1; $Pd/Al_2O_3$, cycle 1). Thus, CO

can be considered a catalyst poison for Pd-containing catalysts.

### *Activity of Pd–M/$Al_2O_3$ (M = Au, Ag, Ce, Cu, Fe, Ni, Co)*

Modification of $Pd/Al_2O_3$ with Au or Ag additives does not lead to the formation of highly active catalysts. This conclusion follows from the low product yields on $Pd–Au/Al_2O_3$ and $Pd–Ag/Al_2O_3$ (Table 1, cycle 1).

At a first glance, the low activity of $Pd–Au/Al_2O_3$ and $Pd–Ag/Al_2O_3$ may be associated with a change in the structure of bimetallic particles under the action of CO released in the side process of ethanal decarbonylation. As is known, the adsorption of CO molecules on Pd–Au and Pd–Ag particles leads to their rearrangement and enrichment of the surface of bimetallic particles with palladium [25–27]. Therefore, under the conditions of the catalytic conversion of ethanol, the Pd–Au and Pd–Ag alloy particles can transform into particles with a core(PdM)–shell(Pd) structure. As a result, $Pd–Au/Al_2O_3$ and $Pd–Ag/Al_2O_3$ can be regarded as structural analogs of the $Pd/Al_2O_3$ catalyst, which is inactive in the conversion of ethanol into α-alcohols, as shown above.

It should be noted, however, that the activity of the Pd–Au and Pd–Ag catalysts observed in the present work is significantly lower than that of the Pd sample. This follows from the product yields on $Pd–Au/Al_2O_3$, $Pd–Ag/Al_2O_3$, and $Pd/Al_2O_3$ in the standard test cycle (cycle 1, Table 1; ω(Pd–Au) = 8.4%, ω(Pd–Ag ) = 4%, and ω(Pd) = 16.5%). In this case, the rate of deactivation of Pd–Au and Pd–Ag in the CO atmosphere is higher than that for the monometallic Pd sample. For example, the following product yields were obtained in the standard test cycle after addition of $1 \times 10^{-4}$ mol of CO into the reactor with ethanol and catalyst: 0.2% for $Pd–Ag/Al_2O_3$ and 1% for $Pd/Al_2O_3$.

Thus, the segregation described in [25–27] can lead to the formation of core(PdM)–shell(Pd) structures. Within this model, however, it is difficult to explain the experimentally observed increase in the deactivation rate of the Pd–Ag and Pd–Au catalysts in the presence of CO and the lower activity of $Pd–Au/Al_2O_3$ and $Pd–Ag/Al_2O_3$ compared with that of $Pd/Al_2O_3$.

The results can be interpreted within the framework of the *d* band theory considered in [13]. It follows from the data of [13] that the interaction of Pd with Au (Ag) leads to a positive displacement of the center of the Pd *d* band by +0.2 (+0.3) eV. As a result, palladium in Pd–Au and Pd–Ag systems becomes more reactive, and the energy of CO binding with Pd increases [13]. The increase in the binding energy of CO with palladium atoms of the metal-containing phase should evidently lead to faster deactivation of the catalyst and hence to lower accumulation rate of α-alcohols during ethanol conversion into α-alcohols, which is just observed in our experiments (Table 1, Fig. 1).

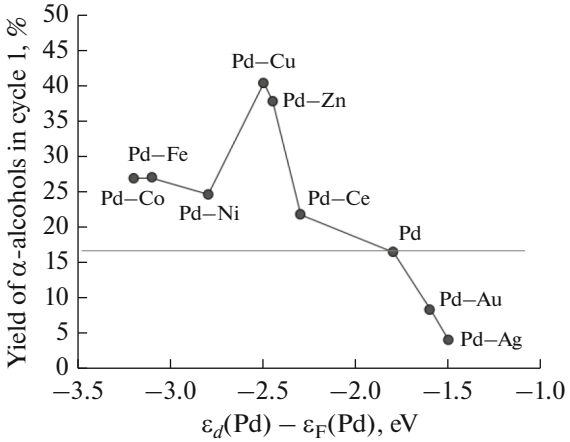


**Fig. 1.** Dependence of the yield of reaction products on the position of the center of the Pd *d* band in the catalysts. $\varepsilon_d$(Pd) is the energy of the center of the Pd *d* band, and $\varepsilon_F$(Pd) is the energy of the Fermi level of palladium.

Modification of $Pd/Al_2O_3$ with Ce, Zn, or Cu additives leads to an increase in the yield of α-alcohols (Table 1), which indicates that the $Pd–Ce/Al_2O_3$, $Pd–Zn/Al_2O_3$, and $Pd–Cu/Al_2O_3$ catalysts are resistant to CO poisoning. This is probably again associated with a shift of the center of the Pd *d* band. As is known, the center of the Pd *d* band in Pd–Ce, Pd–Zn, and Pd–Cu systems is shifted by −0.5, −0.65, and −0.7 eV, respectively, relative to that of pure palladium [13–16]. As a result of the negative shift of the center of the *d* band of Pd, its reactivity decreases [13], which should lead to a decrease in CO sorption on Pd and, as a consequence, to an increase in the yield of α-alcohols. Indeed, according to the data of Table 1 and Fig. 2, the rate of the target process on the $Pd–Ce/Al_2O_3$, $Pd–Zn/Al_2O_3$, and $Pd–Cu/Al_2O_3$ catalysts increases.

In the first cycle of testing, the yield of α-alcohols on $Pd–Cu/Al_2O_3$ is 40%, which is approximately two times higher than during ethanol conversion on $Pd/Al_2O_3$ and does not change during 20 consecutive cycles. The addition of excess CO to the mixture before the start of reaction does not lead to catalyst deactivation either (Table 1). The efficiency of ethanol conversion into α-alcohols observed in the presence of $Pd–Cu/Al_2O_3$ is much higher than that for the catalysts of the target process described in [1–7].

Note that the Pd–Fe, Pd–Co, and Pd–Ni catalysts with a relatively large negative shift of the center of the Pd *d* band (from −1 to −1.4 eV [13]) also do not lose activity in the presence of CO liberated in the reaction and demonstrate stability in repeated cycles (Table 1,

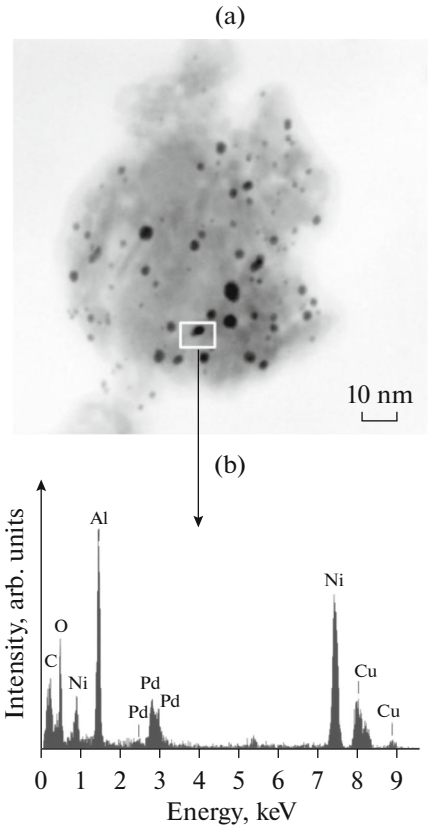


**Fig. 2.** (a) Typical TEM micrograph of the reduced Pd–$Cu/Al_2O_3$ sample and (b) identification of Pd–Cu particles using EDA spectra.

Fig. 1). In contrast to the most efficient Pd–Cu catalyst, the Pd–Fe, Pd–Co, and Pd–Ni systems are characterized by lower yields of the desired product largely because of a decrease in ethanol conversion, rather than a change in the selectivity of formation of α-alcohols (Table 1). Probably, in the case of Pd–Fe, Pd–Co, and Pd–Ni systems, the reactivity of Pd decreases so strongly that this leads to a decrease in sorption and activation of not only CO, but also of ethanol and/or reaction intermediates.

### *Structure of the Active Sites of the Optimum Pd–Cu Catalyst*

$Pd–Cu/Al_2O_3$ was found to be the optimum catalyst for ethanol conversion into α-alcohols; therefore, it was of interest to study the structure of its surface and reconstruct the active sites.

The morphology of the supported phases of the reduced catalyst was studied by TEM. A typical micrograph of $Pd–Cu/Al_2O_3$ is shown in Fig. 2a. The micrograph shows dark rounded particles contrasting with the gray support surface. The EDA spectrum obtained from the location with a single particle contains the C, Al, O, and Ni lines, as well as the Pd and Cu lines. The Ni and C lines are due to the presence of these elements in the TEM grid used for analysis, while the Al and O lines are related to the presence of the $Al_2O_3$ support in the catalyst. The remaining combination of elements (Pd and Cu) unambiguously suggests the bimetallic composition of the analyzed particle (Fig. 2b). The particle size distribution histogram, which has a monomodal shape, is shown in Fig. 3. According to the histogram, the size of the detected particles ranges from 1 to 10 nm. The average particle size is $4 \pm 1$ nm.

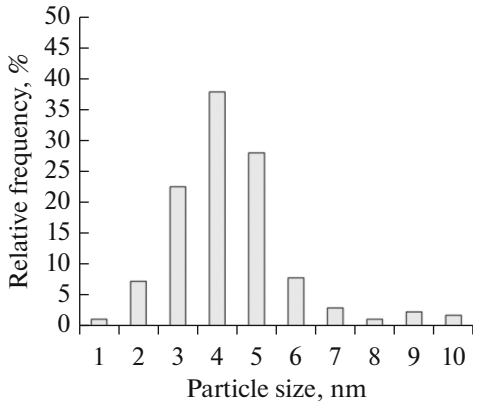


**Fig. 3.** Histogram of particle size distribution in the reduced Pd–$Cu/Al_2O_3$ catalyst.

The TPR-$H_2$ profile of the unreduced PdO–$CuO/Al_2O_3$ sample is shown in Fig. 4. It contains an intense peak at 180°C and two weak peaks at 500 and 750°C. A comparison with the previously obtained profile of the support allows us to conclude that the high-temperature peaks are related to the reduction of transition metal oxide impurities contained in $Al_2O_3$. The peak at 180°C (Fig. 4) is due to the reduction of palladium and copper oxides deposited on the $Al_2O_3$ surface, which are in close contact with each other [28, 29]. Thus, both the TPR-$H_2$ and TEM-EDA data indicate the presence of bimetallic structures in the Pd–Cu catalyst. An analysis of the TPR-$H_2$ profile shows that the temperature used in this study for the reduction of the catalyst with hydrogen before the reaction (200°C) is sufficient for complete reduction of the supported phases of the Pd–Cu catalyst. To verify this, additional XPS studies were performed.

Figure 5 shows the Cu2*p* and Pd3*d* XPS spectra obtained for the reduced Pd–$Cu/Al_2O_3$ catalyst. The absence of "shake-up" satellites in the region of 944 and 963 eV in the Cu2*p* spectrum and intense peaks with electron binding energies of 337.4 and 342.7 eV in the Pd3*d* spectrum indicates that the reduced Pd–Cu sample has no copper ($Cu^{+2}$) and palladium ($Pd^{+2}$) precursor cations. The Cu XPS spectra contain the

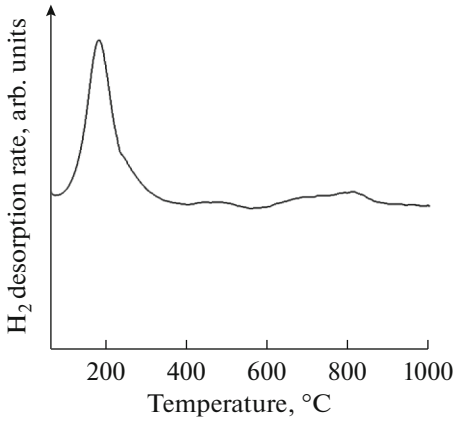


**Fig. 4.** TPR-$H_2$ profile of the unreduced PdO–$CuO/Al_2O_3$ sample.

$Cu2p_{3/2}$ peak with $E_{bnd}$ = 932.8 eV, which indicates that the sample contains the compounds of zero-valent copper [30]. The Pd XPS spectra have a peak $Pd3d_{5/2}$ with an electron binding energy of 335.1 eV, which belongs to the compounds of zero-valent palladium [17, 31]. Thus, the data on the chemical composition of supported metals in the Pd–Cu sample are in good agreement with the previously discussed results of TPR-$H_2$ (Fig. 4). Note that the Pd3*d* peaks in the spectrum of the Pd–Cu catalyst shifted by ~0.2 eV toward lower binding energies relative to those for the $Pd/Al_2O_3$ sample (Fig. 5). According to [28, 32], this effect can be explained by modification of the electronic structure of Pd in the particles of the Pd–Cu alloy. Note that, according to the TEM-EDA data, bimetallic particles are indeed present in the reduced Pd–Cu catalyst.

The TPD-$NH_3$ profile of the reduced Pd–$Cu/Al_2O_3$ catalyst is shown in Fig. 6. It is identical to the TPD-$NH_3$ spectrum of the pure support (Fig. 6) and contains a wide peak of ammonia desorption in the range 200–300°C, which suggests the presence of strong and moderately strong acid sites of the surface according to [6, 33].

Based on the above results, it can be concluded that the Pd–$Cu/Al_2O_3$ surface consists of Pd–Cu particles with a size of 4 ± 1 nm deposited on the $Al_2O_3$ surface. It follows from the data of [1–5] that an effective catalyst for the synthesis of α-alcohols should contain both metal and acid sites of dehydrogenation/hydrogenation (Scheme 1); for the maximum reaction rate, the sites of these two types should be located close to each other [5]. In the Pd–$Cu/Al_2O_3$ catalyst, these conditions are satisfied by bifunctional pairs $Cu^0$–$Al_2O_3$ and $Pd^0$–$Al_2O_3$, which form on the periphery of the supported Pd–Cu particles. As shown in [11],

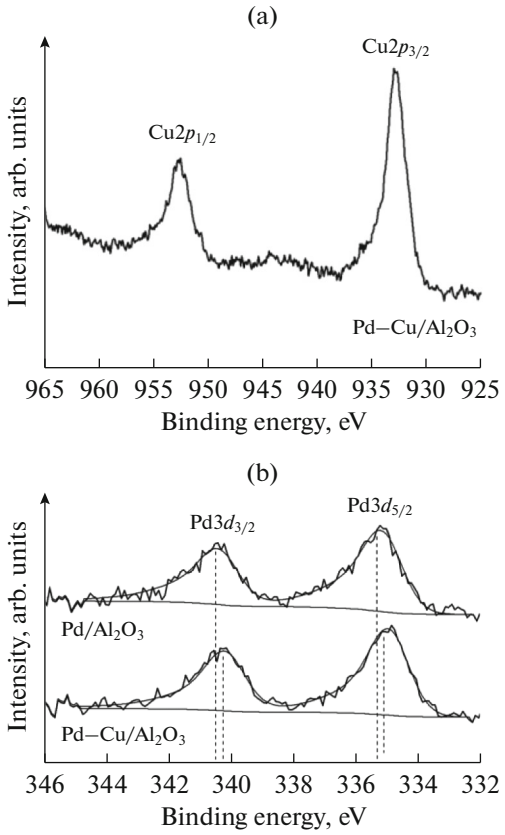


**Fig. 5.** (a) Cu2*p* and (b) Pd3*d* XPS spectra in the reduced Pd–$Cu/Al_2O_3$ sample and $Pd/Al_2O_3$.

however, the $Cu^0$–$Al_2O_3$ vapors exhibit low activity in the process because of the low reactivity of Cu in hydrogenation. Therefore, the most active sites of the Pd–$Cu/Al_2O_3$ catalyst are the $Pd^0$–$Al_2O_3$ pairs, which form in the contact zone between the Pd–Cu particles and the support.

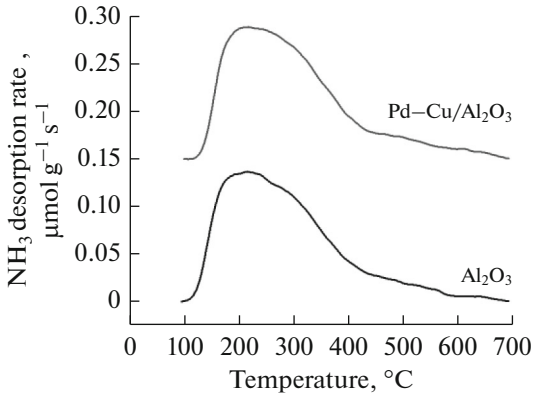


**Fig. 6.** TPD-$NH_3$ profile of the reduced Pd–$Cu/Al_2O_3$ sample and $Al_2O_3$.

## CONCLUSIONS

It was found that the $Pd/Al_2O_3$ monometallic catalyst had high initial activity in the conversion of ethanol into linear α-alcohols. After 10 h of operation, $Pd/Al_2O_3$ lost ~90% of its activity because of deactivation caused by the chemisorption of the CO by-product on active palladium sites.

Modification of $Pd/Al_2O_3$ with Au or Ag additives leads to the formation of less active catalysts, which is consistent with the positive shift of the center of the Pd *d* band in the Pd–Au and Pd–Ag systems and hence with the higher reactivity of palladium with CO. When $Pd/Al_2O_3$ is modified with Cu, Ce, Zn, Fe, Ni, and Co additives, more active catalysts form; this correlates with the negative shift of the center of the Pd *d* band in the Pd–Cu, Pd–Ce, Pd–Zn, Pd–Fe, Pd–Ni, and Pd–Co systems and hence with the lower reactivity of Pd in CO sorption.

Among the bimetallic catalysts under study, the Pd–Cu sample is most efficient in the target process. It is resistant to CO poisoning and allows synthesis of linear α-alcohols from ethanol at 95% selectivity. The stable operation time of the catalyst is at least 100 h. Based on the known reaction mechanism and the TEM, EDA, XPS, TPR-$H_2$, and TPD-$NH_3$ data, the active sites of $Pd–Cu/Al_2O_3$ were reconstructed. The most active sites of the Pd–Cu catalyst were found to be the copper-modified $Pd^0$ metal sites located near the acid-base sites of $Al_2O_3$.

## ACKNOWLEDGMENTS

We are grateful to K.I. Maslakov, S.V. Maksimov, and S.V. Dvoryak (Multiaccess Center "Nanochemistry and Nanomaterials", Moscow State University) for help with studies of the samples using the equipment obtained under the Program of Development of Moscow State University.

## FUNDING

This study was performed under the government contract at the Topchiev Institute of Petrochemical Synthesis, Russian Academy of Sciences.

## REFERENCES

1. Wu, L., Moteki, T., Gokhale, A.A., Flaherty, D.W., and Toste, F.D., *Chem.*, 2016, vol. 1, p. 32.
2. Angelici, C., Weckhuysen, B.M., and Bruijnincx, P.C.A., *ChemSusChem*, 2013, vol. 6, p. 1595.
3. Sun, J. and Wang, Y., *ACS Catal.*, 2014, vol. 4, p. 1078.
4. Gabriëls, D., Hernández, W.Y., Sels, B., Van Der Voort, P., and Verberckmoes, A., *Catal. Sci. Technol.*, 2015, vol. 5, p. 3876.
5. Kozlowski, J.T. and Davis, R.J., *ACS Catal.*, 2013, vol. 3, p. 1588.
6. Marcu, I.-C., Tanchoux, N., Fajula, F., and Tichit, D., *Catal. Lett.*, 2013, vol. 143, p. 23.
7. Riittonen, T., Toukoniitty, E., Madnani, D.K., Leino, A.-R., Kordas, K., Szabo, M., Sapi, A., Arve, K., Wärnå, J., and Mikkola, J.-P., *Catalysts*, 2012, vol. 2, p. 68.
8. Nikolaev, S.A., Tsodikov, M.V., Chistyakov, A.V., Zharova, P.A., Ezzhelenko, D.I., and Shilina, M.I., *Catal. Today*, 2020. (in press). https://doi.org/10.1016/j.cattod.2020.06.061
9. Royer, S. and Duprez, D., *ChemCatChem*, 2011, vol. 3, p. 24.
10. Ellert, O.G., Tsodikov, M.V., Nikolaev, S.A., and Novotortsev, V.M., *Russ. Chem. Rev.,* 2014, vol. 83, no. 8, p. 718.
11. Nikolaev, S.A., Tsodikov, M.V., Chistyakov, A.V., Zharova, P.A., and Ezzgelenko, D.I., *J. Catal.*, 2019, vol. 369, p. 501.
12. Nikolaev, S.A., Chistyakov, A.V., Zharova, P.A., Tsodikov, M.V., Krotova, I.N., and Ezzhelenko, D.I., *Pet. Chem.*, 2016, vol. 56, no. 5, p. 730.
13. Hammer, B. and Nørskov, J.K., *Adv. Catal.*, 2000, vol. 45, p. 71.
14. Che, J., Li, Y., Lu, N., Tian, C., Han, Zh., Zhang, L., Fang, Y., Qian, B., Jiang, X., and Cui, R., *J. Mater. Chem. A*, 2018, vol. 6, p. 23560.
15. Chen, Z.-X., Neyman, K.M., Gordienko, A.B., and Rösch, N., *Phys. Rev. B*, 2003, vol. 68, p. 075417.
16. Lopez, N. and Nørskov, J.K., *Surf. Sci.*, 2001, vol. 477, p. 59.
17. Nikolaev, S.A., Golubina, E.V., and Shilina, M.I., *Appl. Catal., B*, 2017, vol. 208, p. 116.
18. Naumkin, A.V., Vasil'kov, A.Yu., Volkov, I.O., Smirnov, V.V., and Nikolaev, S.A., *Inorg. Mater.*, 2007, vol. 43, no. 4, p. 381.
19. Zanaveskin, K.L., Lukashev, R.V., Makhin, M.N., and Zanaveskin, L.N., *Ceram. Int.*, 2014, vol. 40, p. 16577.
20. Tjurina, L.A., Smirnov, V.V., Potapov, D.A., Nikolaev, S.A., Esipov, S.E., and Beletskaya, I.P., *Organometallics*, 2004, vol. 23, p. 1349.
21. Nikolaev, S.A., Golubina, E.V., Kustov, L.M., Tarasov, A.L., and Tkachenko, O.P., *Kinet. Catal.*, 2014, vol. 55, no. 3, p. 311.
22. Zanaveskin, K.L., Lukashev, R.V., Maslenikov, A.N., Terekhov, A.V., Makhin, M.N., and Zanaveskin, L.N., *Inorg. Mater.*, 2016, vol. 52, no. 8, p. 796.
23. Dik, P.P., Danilova, I.G., Golubev, I.S., Kazakov, M.O., Nadeina, K.A., Budukva, S.V., Pereyma, V.Yu, Klimov, O.V., Prosvirin, I.P., Gerasimov, E.Yu, Bok, T.O., Dobryakova, I.V., Knyazeva, E.E., Ivanova, I.I., and Noskov, A.S., *Fuel*, 2019, vol. 237, p. 178.
24. Chistyakov, A.V., Zharova, P.A., Nikolaev, S.A., and Tsodikov, M.V., *Catal. Today*, 2017, vol. 279, p. 124.

25. Mamatkulov, M., Yudanov, I.V., Bukhtiyarov, A.V., Prosvirin, I.P., Bukhtiyarov, V.I., and Neyman, K.M., *J. Phys. Chem. C*, 2019, vol. 123, p. 8037.

26. Bukhtiyarov, A.V., Prosvirin, I.P., Saraev, A.A., Klyushin, A.Yu., Knop-Gericke, A., and Bukhtiyarov, V.I., *Faraday Discuss.*, 2018, vol. 208, p. 255.

27. Smirnova, N.S., Markov, P.V., Baeva, G.N., Rassolov, A.V., Mashkovsky, I.S., Bukhtiyarov, A.V., Prosvirin, I.P., Panafidin, M.A., Zubavichus, Y.V., Bukhtiyarov, V.I., and Stakheev, A.Yu., *Mendeleev Commun.*, 2019, vol. 29, p. 547.

28. Di, L., Xu, W., Zhan, Z., and Zhang, X., *RSC Adv.*, 2015, vol. 5, p. 71854.

29. Cai, F., Yang, L., Shan, S., Mott, D., Chen, B.H., Luo, J., and Zhong, C.-J., *Catalysts*, 2016, vol. 6, p. 96.

30. Biesinger, M.C., Lau, L.W.M., Gerson, A.R., and Smart, R.St.C., *Appl. Surf. Sci.*, 2010, vol. 257, p. 887.

31. Ivanova, A.S., Slavinskaya, E.M., Gulyaev, R.V., Zaikovskii, V.I., Stonkus, O.A., Danilova, I.G., Plyasova, L.M., Polukhina, I.A., and Boronin, A.I., *Appl. Catal., B*, 2010, vol. 97, p. 57.

32. Sheng, J., Kang, J., Ye, H., Xie, J., Zhao, B., Fu, X.-Z., Yu, Y., Sun, R., and Wong, C.-P., *J. Mater. Chem. A*, 2018, vol. 6, p. 3906.

33. Hu, Z., Li, W.-Z., Sun, K.-Q., and Xu, B.-Q., *Catal. Sci. Technol.*, 2013, vol. 3, p. 2062.

*Translated by L. Smolina*